Catalytic hydrogenation of dimethyl itaconate in non-ionic microemulsions: influence of the size of micelle†‡

Juan Milano-Brusco,[a] Sylvain Prévost,[bc] Dersy Lugo,[b] Michael Gradzielski[b] and Reinhard Schomäcker*[a]

Received (in Montpellier, France) 12th March 2009, Accepted 30th April 2009
First published as an Advance Article on the web 2nd June 2009
DOI: 10.1039/b905063a

The structural dimensions of two different microemulsions were extracted and correlated with the catalytic hydrogenation of dimethyl itaconate (DMI) performed in such media using the water-soluble catalyst complex Rh–TPPTS. The commercial, polyoxyethylene-based non-ionic surfactants Igepal CA-520 and Triton X-100 were used to obtain two different types of microemulsions with cyclohexane and water; pentanol as a cosurfactant was added to the Triton system. Dynamic light scattering (DLS) and small angle neutron scattering (SANS) measurements were used to determine the characteristic sizes of the Igepal and Triton microemulsions, respectively, showing a linear dependence between the initial hydrogenation rate of DMI and the radius of the micelles. The initial hydrogenation rate of DMI in bulk water is exceeded in both microemulsions. Indications of deformation of the originally spherical Triton X-100 reverse micelles upon addition of the water-soluble catalyst complex Rh–TPPTS were found.

1. Introduction

Micelles are supramolecular assemblies in a colloidal dimension. These assemblies are based on the amphiphilic characteristics of surfactants or amphiphiles, which are molecules with a polar head group and a hydrophobic tail. Micelles can be formed in water and in non-polar solvents (see Scheme 1), for which the names of micelles and reverse micelles have been given, respectively. Reverse micelles are formed by the association of polar head groups of amphiphiles with colloidal drops of water in an organic medium once the concentration of the amphiphiles in the interface is appropriate.[1,2] The delimitation of hydrophilic and hydrophobic micro-domains is an important feature of reverse micelles favourable to reactions.[3] For this reason they are being regarded as microreactors, whose capacity for reactants and variability of solubilization properties are high and of practical interest.[4] Contrary to the case of aqueous micelles, reactions in reverse micelles are possible at high concentrations of hydrophobic substrates, and in regard to homogeneous reaction media they can be divided, as observed in Scheme 1, into three spatial domains: the aqueous core, the hydrophilic–hydrophobic interface, and the surrounding hydrophobic medium. Water in the core may display deviating electrophilic and nucleophilic properties relative to "bulk water" because of strong interactions with the head groups of the surfactant, depending on the size of the droplets. Thus, the effect of this medium on reaction rates is often dependent on the water/surfactant (ω) molar ratio.[5]

We have recently published a kinetic study that compares the catalytic hydrogenation of dimethyl itaconate in a Triton X-100 microemulsion and in a biphasic system.[6] In this study we noticed an important influence of the microemulsion formulation on the initial rate of the hydrogenation. The Triton X-100 system used in the earlier study needed the addition of 1-pentanol as cosurfactant, which also had an inhibition effect on the hydrogenation. Cosurfactants are used in order to stabilize the surfactants in the interface. When the amphiphile molecules have large polar groups, as Triton X-100 has,[7] the interactions between each surfactant molecule destabilize the micelle. For this reason the addition of short-chain alkanols, which also have amphiphilic properties and position themselves in between the surfactant molecules, cushion the interactions stabilizing the micelles.[6,8] The cosurfactant has also an important effect on the size of the micelles. Accordingly the determination of the size and the structural characterization of the microemulsion droplets is an important aspect in understanding catalytic reactions in

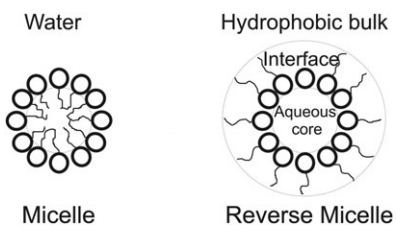

Scheme 1 Scheme of a micelle and a reverse micelle.

[a] *Department of Chemistry, TU Berlin, Secr. TC-8, Strasse des 17. Juni 124, 10623 Berlin, Germany. E-mail: schomaecker@tu-berlin.de*
[b] *Stranski Laboratorium für Physikalische und Theoretische Chemie, Department of Chemistry, TU Berlin, Secr. TC-7, Strasse des 17. Juni 124, 10623 Berlin, Germany*
[c] *Helmholtz Zentrum Berlin, Glienicker Strasse 100, 14109 Berlin, Germany*

† This article is warmly dedicated to Professor Dr G. H. Findenegg on the occasion of his 70th birthday.

‡ Electronic supplementary information (ESI) available: Original data from the cosurfactant partitioning study (Table A, B & C), preliminary data for the analysis of the SANS measurements (Table D, E & F), and autocorrelation functions for the DLS measurements (Fig. A & B). See DOI: 10.1039/b905063a

microemulsions. Due to the small size of the micelles, whose diameters are typically in the range of 1–100 nm,[9,10] microemulsions are usually transparent; this characteristic feature has rendered them amenable for studies by dynamic light scattering (DLS).[10,11] Such studies are accurate when the samples are highly diluted, enough to safely neglect interactions between aggregates and multiple scattering. This condition is often not satisfied with microemulsions.[12] Hence experiments and data analysis applying the scattering theories must be performed with special care, and the results must be regarded with a critical mind and be combined with results from other techniques. In contrast to DLS, small angle neutron scattering (SANS) with its higher spatial resolution can be applied to such systems to corroborate values obtained for the hydrodynamic radius and add information regarding the core size of the micelles. Small angle neutron scattering (SANS) is a well established technique used to characterize microemulsions in much structural detail,[13–19] and it has been successfully applied to Triton X-100 micellar systems.[20,21]

The present study reports the correlation between the size of reverse micelles obtained by SANS and DLS, and the initial hydrogenation rate of dimethyl itaconate (DMI) with the water-soluble catalyst complex Rh–TPPTS using two non-ionic microemulsion systems with different water content (characterized by ω) as dispersive media. In addition, the influence of the cosurfactant–surfactant mass ratio (δ) as a reaction parameter was studied.

2. Experimental section

2.1 Chemicals

The solvents cyclohexane ($\geq$ 99.5%, Roth) and 1-pentanol ($\geq$ 99%, Merck) were degassed and purged under nitrogen and used without further purification. Cyclohexane-d_{12} (99.5%, Deutero GmbH), deuterium oxide (99.9%, Deutero GmbH), poly(ethylene glycol) 400 and 1000 (100%, Fluka), the water-soluble ligand TPPTS (30.7 wt% in water, Celanese), and the surfactants Triton X-100 (100%, Sigma-Aldrich) and Igepal CA-520 (100%, Sigma-Aldrich) were used as received. The catalyst precursor $[Rh(cod)Cl]_2$ (98%, Strem) was kept under nitrogen and used as received.

2.2 Microemulsion preparation

The following common terms were used to describe the compositions of the four-component systems; these terms are simplified in case of using a three-component system (without cosurfactant):

$$\alpha = \frac{m_{oil}}{m_{oil} + m_{water}}$$

$$\gamma = \frac{m_{surfactant}}{m_{oil} + m_{water} + m_{surfactant}}$$

$$\delta = \frac{m_{cosurfactant}}{m_{surfactant}} \qquad (1)$$

$$\omega = \frac{n_{water}}{n_{surfactant}}$$

$$\omega_T = \frac{n_{water}}{n_{surfactant} + n_{cosurfactant}}$$

where m indicates the mass and n the number of moles.

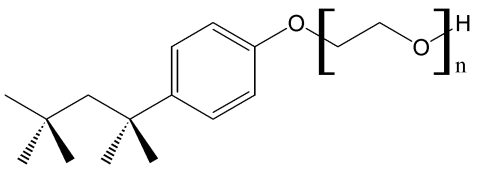

Scheme 2 (*p*-*tert*-Octylphenoxy)polyethoxyethanol chemical formula.

The surfactants used were the commercially available Triton X-100 and Igepal CA-520, respectively. Both are based on *tert*-octylphenoxypolyethoxyethanol (Scheme 2) with different number of ethoxyethanol groups. Igepal CA-520 has approximately half the ethoxyethanol groups (n = 5) of Triton X-100 (n = 9–10).

Test tubes were prepared with different compositions of water and cyclohexane (α) but fixed weight fractions of Triton X-100 and 1-pentanol (γ). The sequence in which the components were added was: (1) cyclohexane, (2) Triton X-100, (3) 1-pentanol, and (4) water. Before and after water addition, the solution was agitated for 5 min. The test tubes were immersed in a thermostated water bath, and phase behaviour was observed after 15 min. This procedure was repeated with increasing temperature of 1 K stepwise. The same procedure was used for the Igepal CA-520 system. The change in phase behaviour depending on temperature and composition followed a pattern typical for non-ionic surfactant-based microemulsions.

2.3 Cosurfactant partition

Many publications dealing with microemulsion quaternary systems take into consideration that the cosurfactant, which in our case is 1-pentanol, partitions itself between the interfacial film and the continuous oily phase.[12,22,23] We wanted to start by analysing the percentage of pentanol possibly accumulated in the core of the micelles. For this reason, a partition study of 1-pentanol in biphasic systems cyclohexane–water with PEG 400, cyclohexane–water with PEG 1000 and cyclohexane–water alone was made. The compositions for the Triton X-100 systems shown in Table 1 were used to prepare the samples, and instead of adding Triton X-100, the same molar amount of PEG was added. PEG 400 represents a good approximation for the polar group of the Triton X-100 molecules, and the cyclohexane–water systems with and without PEG 1000 allows us to observe the influence of PEG and its ethoxyethanol chain length on the pentanol partition. The pentanol concentration in the cyclohexane phase was analysed by gas chromatography (GC) using a Shimadzu 2010 GC (DB-5HT column, approx. 30 m, d = 0.32 mm, 0.4 bar N_2, 70 °C, FID) obtaining a retention time for 1-pentanol of approximately 3 min.

2.4 Catalytic hydrogenation runs

The hydrogenation of DMI catalysed by the water-soluble catalyst complex Rh–TPPTS (Scheme 3) was selected as a reference for studying the influence of the micelle size on the reaction kinetics. DMI has a partition coefficient smaller than 1 at low DMI concentrations (<50 mmol L^{-1}) in a cyclohexane–water biphasic system, but by increasing the DMI concentration to higher values (>50 mmol L^{-1}) more

Table 1 Composition of the different microemulsions for both systems: [Triton X-100–1-pentanol]–cyclohexane–water and Igepal CA-520–cyclohexane–water

Sample	Surfactant[a]	α	γ (%)	ω	ω_T	δ
ME 1	Triton X-100	0.94	10	20.0	3.10	0.75
ME 2	Triton X-100	0.95	10	15.0	2.31	0.75
ME 3	Triton X-100	0.97	10	10.0	1.54	0.75
ME 4	Triton X-100	0.94	10	20.0	2.42	1.00
ME 5	Triton X-100	0.95	10	15.0	1.80	1.00
ME 6	Triton X-100	0.97	10	10.0	1.20	1.00
ME 7	Triton X-100	0.94	10	20.0	1.98	1.25
ME 8	Triton X-100	0.95	10	15.0	1.47	1.25
ME 9	Triton X-100	0.97	10	10.0	0.98	1.25
ME 10	Triton X-100	0.94	10	20.0	1.68	1.50
ME 11	Triton X-100	0.95	10	15.0	1.25	1.50
ME 12	Triton X-100	0.97	10	10.0	0.83	1.50
ME 13	Igepal CA-520	0.956	3.36	30.0	—	—
ME 14	Igepal CA-520	0.956	3.70	27.5	—	—
ME 15	Igepal CA-520	0.956	4.00	25.0	—	—
ME 16	Igepal CA-520	0.956	4.40	22.5	—	—
ME 17	Igepal CA-520	0.956	5.00	20.0	—	—
ME 18	Igepal CA-520	0.956	3.30	30.6	—	—
ME 19	Igepal CA-520	0.960	3.30	27.5	—	—
ME 20	Igepal CA-520	0.964	3.30	25.0	—	—
ME 21	Igepal CA-520	0.968	3.30	22.5	—	—

[a] For the reactions, all the microemulsions were prepared with cyclohexane and water. For the Triton X-100 system, 1-pentanol was used as cosurfactant.

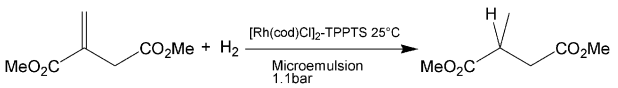

Scheme 3 Hydrogenation of dimethyl itaconate formal reaction.

DMI accumulates in the cyclohexane phase and the partition coefficient becomes higher than 1. This partition behaviour can be influenced by the presence of surfactants in the solution, changing the apparent order of the reaction from zero in a biphasic system to one in microemulsions.[6]

First, the catalyst complex was prepared by mixing 22 mg of the catalyst precursor $[Rh(cod)Cl]_2$ (0.089 mmol Rh) with 1240 mg aqueous 30% TPPTS solution (380.4 mg, 0.67 mmol TPPTS) under nitrogen. This mixture was stirred under nitrogen at ambient temperature for 24 h before it was used in the hydrogenation reaction. The high molar ratio of TPPTS/Rh (7.5) is used to ensure that the hydrogenation starts at a maximal reaction rate and to avoid the formation of rhodium metal.[6] A thermostated double wall 200 ml glass reactor equipped with a gas dispersion stirrer was used in this study. Semi-batch reactions were performed under a constant hydrogen pressure of 1.1 bar. The reaction rates were calculated using the monitored hydrogen flow rate for keeping the pressure at a constant level.

The microemulsions were prepared one day before the experiment and agitated overnight. The reactor was evacuated at 150 mbar and refilled with nitrogen 3 times after introducing the solvent and again after injection of the catalyst solution (1.2 g) and 2 g of DMI, respectively. The mixture was stirred at 400 rpm and 40 °C for 30 min and afterwards at reaction temperature for 30 min. The reaction was initiated after evacuating the reactor to 150 mbar, followed by an increase in the pressure to 1.1 bar with hydrogen gas and subsequent stirring at 800 rpm. A decreasing and finally expiring hydrogen flux indicated the end of the reaction. The complete hydrogenation of DMI to dimethyl methylsuccinate (DMS) was confirmed by gas chromatography (GC) using a HP 5710A instrument (Lipodex E capillary column, *ca.* 25 m, d = 0.25 mm, 0.6 bar N_2, 90 °C, FID) obtaining a retention time of DMS of approximately 20 min. Microemulsion samples were separated into organic and aqueous phases by addition of water. After phase separation the organic phase was analysed. Table 1 shows the compositions of the different microemulsions used as media for the hydrogenation experiments.

2.5 Dynamic light scattering

All samples were measured without catalyst. Dynamic light scattering (DLS) was employed in order to study the size of the micelles of the Igepal CA-520 systems in terms of the hydrodynamic radius. Correlation functions were recorded at a scattering angle of 90° using a typical ALV goniometer setup with a Nd:YAG-laser as light source (wavelength λ = 532 nm). The constant output power was 150 mW. All measurements were done at 25 °C controlled by a toluene matching bath. The correlation functions were generated using an ALV-5000/E multiple τ digital correlator and finally analysed by inverse Laplace transformation (CONTIN).[24]

2.6 Small angle neutron scattering

SANS spectra were recorded on the instrument V4 at the BER reactor of the Helmholtz Zentrum Berlin, Germany. Data were recorded on a 64 × 64 2-dimensional gas detector (128 × 128 pixels), at a constant wavelength of 6.3 Å (FWHM 18%). Samples were filled into a quartz cuvette (QS, Hellma) with a neutron path length of 1 mm and thermostated at 25.3 °C ± 0.4. Three sample-detector distances were used: 1, 4, 12 m, with collimation at 2, 4 and 12 m, respectively. Data reduction was performed using the software package BerSANS, with correction from the scattering contribution of the empty cell, and deviations in the pixel efficiency accounted for using the incoherent scattering of a 1 mm pure water sample. Electronic and ambient background was accounted for by the measurement of a cadmium plate. The transmission of water was used to obtain the instrumental coefficient, assuming the ideal case where non-transmitted neutrons are scattered uniformly over the full solid angle (4π). Finally data were azimuthally averaged, and intensities at different configurations but corresponding to the same sample were merged without the need of a scaling factor. Due to the fact that the interactions of neutrons with hydrogen and deuterium are widely different, labelling the microdomains of the micelles with deuterated compounds is possible.[25] For this reason, different contrast conditions were used: microemulsions were prepared from heavy water, Triton X-100, 1-pentanol, and either hydrogenated or perdeuterated cyclohexane. The former case provides an inner look at the D_2O-based core of the micelles, while in the latter case the hydrogenated interfacial film is probed. Two different methods were used to calculate the hydrodynamic radius, both using the parameters obtained by the Guinier

approximation.[15] The Guinier approximation has the following form:

$$I(q) = I_0 \exp\left[-\frac{q^2 R_g^2}{3}\right] \quad (2)$$

where I_0 is the absolute intensity and R_g is the radius of gyration. R_g is determined with linear regressions on Guinier plots ($\ln(I)$ *vs.* q^2) of the SANS data, and the radius of the corresponding homogeneous spheres is estimated following the form:

$$R_{g_{Sph}}^2 = \tfrac{3}{5}R^2 \quad (3)$$

Small angle neutron scattering theory allows for another basic way of determining the radius of the micelles, namely the coherent macroscopic scattering cross section from an assembly of particles dispersed in a solvent. The macroscopic scattering cross section is represented by the expression given below:[25]

$$I(q) = \phi \Delta p^2 V_p F(q) S(q) \quad (4)$$

where ϕ is the volume fraction of particles, V_p their volume, Δp the contrast, $F(q)$ is the form factor accounting for the shape and size of particles and $S(q)$ is the structure factor accounting for the spatial correlation between particles.

By considering the micelles to be non-interactive in a dilute solution ($S(q) = 1$) and extrapolating to zero q ($F(q) = 1$), eqn (4) can be re-arranged and gives:

$$V_p = \frac{I_0}{\phi \Delta p^2} \quad (5)$$

ϕ is calculated with the volume fractions of the polar components:

$$\phi = \phi_{EO_{10}} + \phi_{H_2O} + \phi_{D_2O} + (x_{C_5H_{12}O}\phi_{C_5H_{12}O}) \quad (6)$$

where $\phi_{EO_{10}}$, ϕ_{H_2O}, ϕ_{D_2O} and $\phi_{C_5H_{12}O}$ are the volume fractions of the polar part of Triton X-100, water attached to the ethoxy chain of the surfactant, deuterium oxide and pentanol, respectively, and x_{C5H12O} is the fraction of pentanol inside the core of the micelles. The contrast is the difference between the scattering length densities (SLD) of the medium composed of cyclohexane-d_{12} and a fraction of pentanol and the mostly hydrogenated particles using the following equation:

$$\Delta p = \frac{\sum \mathrm{SLD}_{\mathrm{polar}_i}\phi_{\mathrm{polar}_i}}{\sum \phi_{\mathrm{polar}_i}} - \frac{\sum \mathrm{SLD}_{\mathrm{nonpolar}_i}\phi_{\mathrm{nonpolar}_i}}{\sum \phi_{\mathrm{nonpolar}_i}} \quad (7)$$

The software package *SASfit*, written by Joachim Kohlbrecher (Paul-Scherrer Institute, Switzerland), was used to analyse the SANS spectra.

2.7 Conductivity

A commercially available compact conductivity meter cond 330i (WTW, Weilheim, Germany) was used. All conductivity measurements were done at 25 °C.

3. Results and discussion

3.1 Microemulsions

Since Kahlweit and Strey presented for the first time the phase prism for ternary water–oil–surfactant systems,[26] built up from different Gibbs diagrams of the ternary system at different temperatures, studies in this area that dealt with different applications of microemulsions have mainly used two vertical sections of this prism, as seen in Fig. 1, which result in pseudo-binary phase diagrams.[27,28] One section with the temperature as ordinate is obtained by keeping the oil-to-water ratio constant (usually at $\alpha = 0.5$), the other by keeping the amount of surfactant constant. This last diagram shows two biphasic system areas, separated by a horizontal one phase canal. Fig. 2 shows a part of the one phase canal for two systems: (a) [Triton X-100–1-pentanol]–cyclohexane–water and (b) Igepal CA-520–cyclohexane–water. Both systems were studied at surfactant concentrations (γ) of 5 and 10%, respectively, showing the typical behaviour for such systems of a wider one phase canal when using higher concentrations of surfactants. 1-Pentanol was added to the Triton X-100 system in order to stabilize the reverse micelles,[29] as the larger EO group of the Triton X-100 yields a smaller packing parameter that is increased by the addition of the pentanol. In addition the presence of pentanol, as will be shown further, also has an important influence on the DMI hydrogenation catalysed by the water-soluble catalyst complex Rh–TPPTS included in the reverse micelles.

3.2 DMI hydrogenation in microemulsion

Using the compositions from Table 1 for 100 mL of microemulsion, and hydrogenating 2 g of DMI with 20 mg of $[Rh(cod)Cl]_2$ and 346 mg of TPPTS for each microemulsion, a course of hydrogen consumption rate ($[dV(H_2)\ dt^{-1}]$, mL min^{-1}) *versus* time (min) is obtained. The maximum hydrogenation rate observed after stabilization of the pressure control system is taken as the initial rate of the hydrogenation ($[dV(H_2)\ dt^{-1}]_0$, mL min^{-1}). Fig. 3 shows the monitored hydrogen consumption rate when hydrogenating 2 g of DMI in microemulsion ME 1 containing Triton X-100; the initial hydrogenation rate is 5.9 mL_{H_2} min^{-1}.

By increasing the amount of water inside the reverse micelles relative to the amount of surfactant (ω) the initial

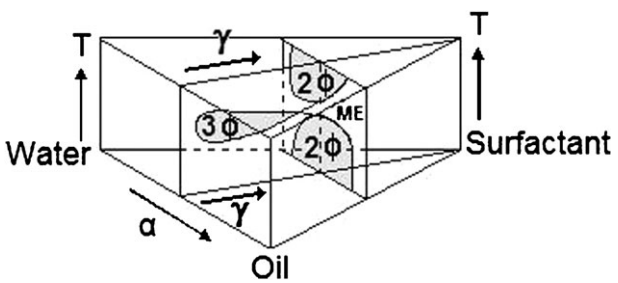

Fig. 1 Schematic phase prism of a ternary mixture of water–oil–surfactant including two characteristic sections at constant α and constant γ, and whose distinctive regions of one phase microemulsion (ME), biphasic (2ϕ) and three-phase system (3ϕ) are observed as a function of the temperature (T).

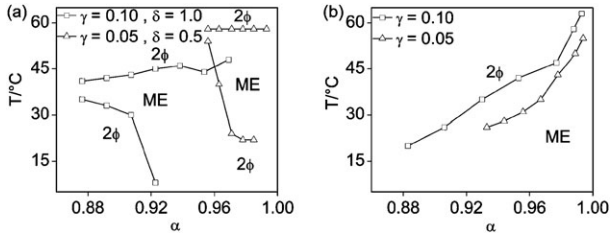

Fig. 2 Phase prism section (constant γ) with the respective one phase microemulsion (ME) and biphasic system (2ϕ) regions of: (a) the quaternary system [Triton X-100–1-pentanol]–cyclohexane–water with two constant weight fractions of Triton X-100 and 1-pentanol, and (b) the ternary system Igepal CA-520–cyclohexane–water with two constant weight fractions of Igepal CA-520.

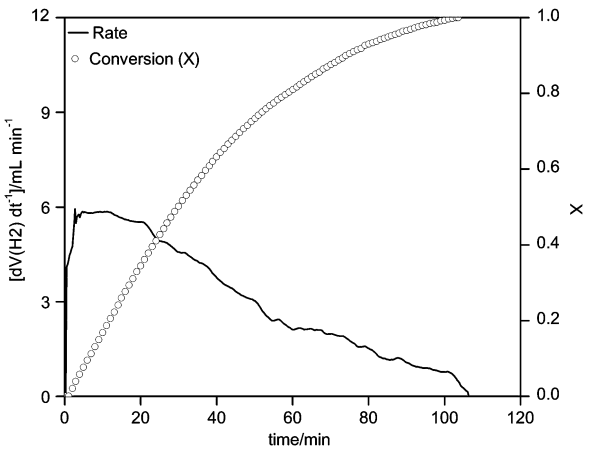

Fig. 3 Hydrogen flux *vs.* time and conversion *vs.* time in the hydrogenation of 2 g of DMI in a microemulsion system constituted by 4.27 g of water, 64.23 g of cyclohexane, 7.61 g of Triton X-100 and 5.71 g of 1-pentanol (ME 1 in Table 1), at 25 °C and 1.1 bar, using 20 mg of $[Rh(cod)Cl]_2$ and 357 mg of TPPTS.

hydrogenation rate of DMI increases. This influence is linearly dependent for all systems as can be seen in Fig. 4. For the Igepal CA-520 systems, also an influence of the surfactant

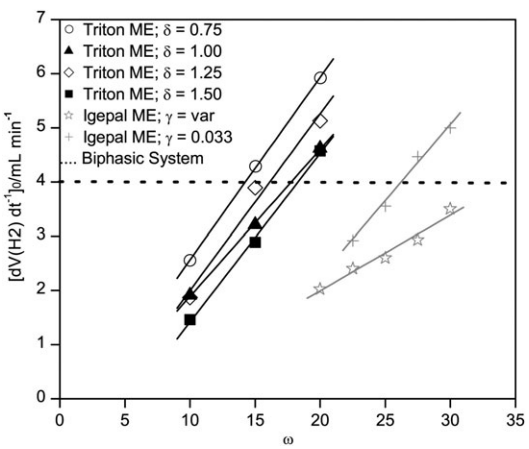

Fig. 4 Initial hydrogenation rate of the catalytic hydrogenation of DMI (2 g in 100 ml of microemulsion) as a function of ω in Triton X-100 microemulsions with different δ, and in Igepal CA-520 microemulsions with γ as a constant and as a variable, at 25 °C and 1.1 bar, using 20 mg of $[Rh(cod)Cl]_2$ and 357 mg of TPPTS.

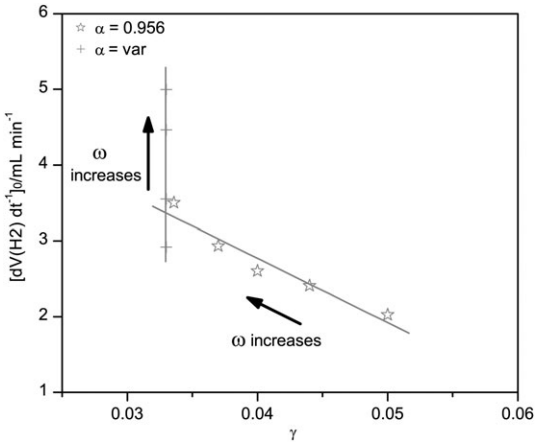

Fig. 5 Initial hydrogenation rate of the catalytic hydrogenation of DMI (2 g in 100 ml of microemulsion) as a function of γ in Igepal CA-520 microemulsions with α as a constant and as a variable, at 25 °C and 1.1 bar, using 20 mg of $[Rh(cod)Cl]_2$ and 357 mg of TPPTS.

concentration is noticeable. As Fig. 5 shows, there are two different patterns described in this figure. First, by decreasing the concentration of Igepal CA-520 (γ) with a constant ratio cyclohexane-to-water ($\alpha = 0.956$), the initial hydrogenation rate increases. Second, by keeping the concentration of Igepal CA-520 constant ($\gamma = 0.033$) with decreasing ratio cyclohexane-to-water (α), the initial hydrogenation rate also increases. Both patterns are proof of an increase of the initial hydrogenation rate with increase of the molar ratio of water to surfactant (ω). Fig. 5 also shows that by comparing the initial hydrogenation rate of DMI in Igepal microemulsions of equal ω from both patterns, the Igepal microemulsions with lower concentration of surfactant ($\gamma = 0.033$) allowed for higher initial hydrogenation rates. By keeping the ratio ω constant, with higher concentrations of Igepal, we expect an increase in the concentration of micelles of equal size, so the catalyst should distribute itself over more micelle cores. For the Triton X-100 microemulsions, by increasing the amount of cosurfactant in relation to the amount of surfactant (δ), the initial hydrogenation rate for each ω decreases, resulting in a displacement of the linearly dependent curves to smaller initial hydrogenation rates, at constant slope (except for $\delta = 1$). This behaviour indicates a direct proportionality between ω and the initial hydrogenation rate within an even wider ω range than shown in Fig. 4 (ω = 10–20), where adding pentanol means an additional amount of surfactant is available for stabilizing the reverse micelles. For this reason the pentanol was also taken into account for the correlation of the initial hydrogenation rate of DMI *vs.* ω_T (Fig. 6).

A model of the micelle is represented in Scheme 4. The three domains observed in this scheme should not be well defined in our microemulsions as the polar chains of Triton X-100 and Igepal CA-520 are rather long.

The results from the partitioning study of pentanol between cyclohexane and water, cyclohexane and an aqueous solution of PEG-400, and the same oil and an aqueous solution of PEG-1000 are shown in Table 2, and the original data for the partitioning study of pentanol is presented in Tables SA, SB

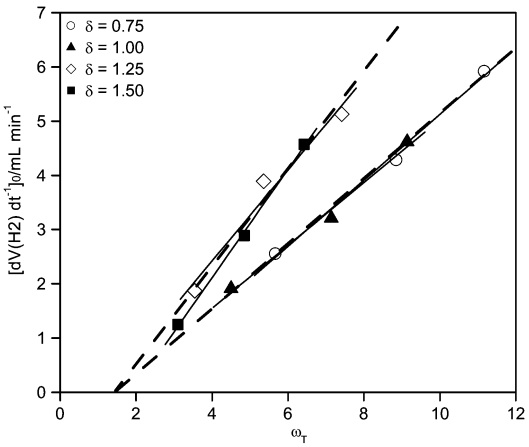

Fig. 6 Initial hydrogenation rate of the catalytic hydrogenation of DMI (2 g in 100 ml of microemulsion) as a function of ω_T in Triton X-100 microemulsions with different δ, at 25 °C and 1.1 bar, using 20 mg of $[Rh(cod)Cl]_2$ and 357 mg of TPPTS.

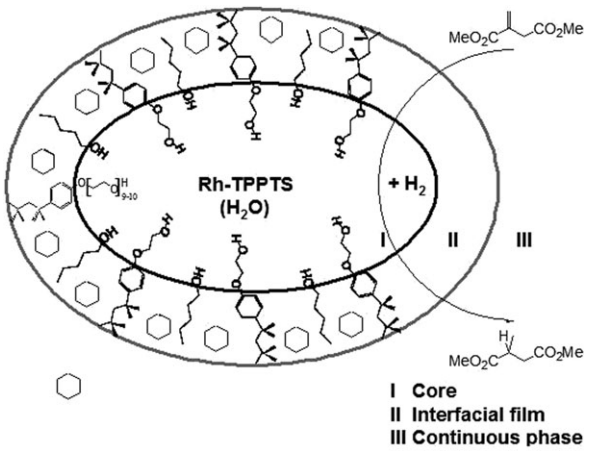

Scheme 4 Ellipsoidal micelle model.

and SC of the ESI.‡ As we observe in Table 2, the percentage of pentanol in the water phase increases when PEG is added and when the ethoxy chain length is increased. This effect of PEG on the partition of pentanol in cyclohexane–water biphasic systems is a simple representation of the effect of the surfactant in our system. The tendency of the polar part of the surfactant Triton X-100 to introduce pentanol inside the core of the micelles is complex, because it is limited by the solubility of the aliphatic chain of 1-pentanol in the interfacial layer and the continuous phase of the microemulsion. For this reason and in order to simplify our pentanol partition calculations, in the following we assume those values in Table 2 (for PEG 400) to represent the amount of pentanol ascribed to the interfacial region, acting as a cosurfactant; the remaining part is therefore diluted in the continuous phase. As we show further in the paper, with this assumption results of micellar volume using the macroscopic scattering cross section are consistent with the micellar volume calculated using the Guinier approximation for ellipsoidal micelles. In Fig. 6, the curves with $\delta \leq 1$ are overlapped and require higher ratios ω_T, to achieve similar initial hydrogenation rates to the curves with $\delta > 1$, which also are overlapped. By adding a smaller amount of surfactant and controlling the water percentage similar initial hydrogenation rates can be achieved. The two groups of overlapped curves show two different patterns, which could be explained by the size and the geometry of the micelles. The extrapolation of the four curves reaches the same point of zero initial hydrogenation rate ($[dV(H_2)\,dt^{-1}]_0 = 0\ mL_{H_2}\ min^{-1}$) at a ω_T of 1.5. This result was experimentally confirmed by hydrogenations using the four systems with different δ, which exhibit zero activity.

3.3 Igepal CA-520 micelles—structural characterization

DLS measurements of the Igepal CA-520 microemulsions of compositions reported in Table 1 could be performed successfully for γ down to 3.36%. With γ = 3.30% results were poorly reproducible, and as one observes in Table 3 (ME 18–21), the measured radii of the micelles fluctuate without any significant pattern. This behaviour could be explained by the closeness to the cloud point of the system and for this reason they are not taken into account in the following discussion. For higher values of γ the microemulsions are relatively monodisperse. A linear dependence of the initial hydrogenation rate to the hydrodynamic radius of the micelles was obtained, which can be represented by the following equation of a line:

$$\left[\frac{dV(H_2)}{dt}\right]_0 = 1.07 + 24.27r \qquad (8)$$

Table 2 Cosurfactant partitioning: molar percentage (%) of 1-pentanol concentrated in the aqueous phase of a biphasic system PEG400–cyclohexane–water at 25 °C, using the compositions from Table 1 for Triton X-100 microemulsions with PEG 400 instead of Triton X-100

Sample	$C_5H_{12}O_{without\ PEG}$[a] (%)	$C_5H_{12}O_{PEG\text{-}400}$[a] (%)	$C_5H_{12}O_{PEG\text{-}1000}$[a] (%)
ME 1	11.67	14.62	20.56
ME 2	9.49	12.65	22.85
ME 3	10.65	13.89	28.25
ME 4	13.93	16.43	27.34
ME 5	12.11	15.00	25.08
ME 6	13.39	16.65	27.79
ME 7	14.87	18.75	21.42
ME 8	17.09	19.63	21.10
ME 9	15.25	19.77	29.09
ME 10	18.45	19.42	24.94
ME 11	18.40	19.04	21.76
ME 12	16.49	20.27	30.01

[a] Concentration of pentanol in the aqueous phase.

Table 3 Radii of the Triton X-100 micelles, volume of the micelles (V_{Sph}) calculated with the Guinier approximation for homogeneous spheres and (V_{Ellip}) for homogeneous ellipsoids using SANS scattering measurements of the Triton X-100 microemulsions, absolute intensity (I_0), volume of the Triton X-100 micelles (V_{I_0}) calculated with the coherent macroscopic scattering cross section assuming all the cosurfactant is concentrated in the continuous phase, and radii of the Igepal CA-520 micelles estimated from DLS measurements of the Igepal CA-520 microemulsions at 25 °C

Sample	r_{R_g}/nm	V_{Sph}/nm^3	V_{Ellip}/nm^3	I_0/cm^{-1}	V_{I_0}/nm^3
ME 1	14.4	12588.94	2670.19	138.61	2046.17
ME 2	7.0	1429.35	947.79	37.13	461.91
ME 3	4.3	332.39	323.63	18.42	191.24
ME 4	9.2	3216.55	1437.86	55.10	952.51
ME 4[a]	13.0	—	—	—	—
ME 4[b]	7.1	—	—	—	—
ME 5	6.5	1152.32	817.48	28.97	412.88
ME 6	4.2	306.02	289.13	15.15	177.14
ME 7	8.2	2332.92	1035.23	43.25	884.29
ME 8	6.5	1125.36	767.15	25.23	411.91
ME 9	3.5	183.01	170.00	9.45	124.41
ME 10	7.2	1575.70	752.19	34.60	823.00
ME 11	5.7	754.56	588.35	21.76	408.25
ME 12	4.5	383.53	282.86	11.38	168.28
ME 13[c]	23.5	—	—	—	—
ME 14[c]	19.0	—	—	—	—
ME 15[c]	16.3	—	—	—	—
ME 16[c]	14.3	—	—	—	—
ME 17[c]	12.0	—	—	—	—
ME 18[c]	18.9	—	—	—	—
ME 19[c]	35.5	—	—	—	—
ME 20[c]	43.0	—	—	—	—
ME 21[c]	38.9	—	—	—	—

[a] ME 4 with D_2O and cyclohexane-d_{12}, 0.8 mmol L^{-1}_{Rh} using a P/Rh ratio of 7.5. [b] ME 4 with D_2O. [c] Radii were measured using DLS.

where $[dV(H_2)\ dt^{-1}]_0$ is the initial hydrogenation rate in mL min^{-1} and r is the hydrodynamic radius in nm.

As observed in Table 3, the obtained radii are significantly larger than the length of the fully extended Igepal CA-520 molecule containing 14 C–C bonds, 11 C–O bonds, a benzene ring, and an O–H bond. The radii are larger than 12 nm, hence this could mean that a water pool is formed. Another possible explanation is that, because DLS measurements have no means of determining geometrical deformations and it only allows for the determination of an effective hydrodynamic radius, the micelles could be elongated. By doubling the radius from 12 to 24 nm the initial hydrogenation rate of DMI almost doubles as well: from 2 to 3.5 mL_{H_2} min^{-1}. Investigations of AOT microemulsions have shown that the properties of the water are modified as the water content in the microemulsion varies, reaching properties similar to bulk water for high values of ω in the microemulsions.[30,31] We found earlier that the initial hydrogenation rate of DMI in a biphasic system cyclohexane–water, in which the water properties are those of bulk water, is approximately 4 mL_{H_2} min^{-1}.[6] Plots of the autocorrelation functions $g^2(\tau)$ are available as ESI‡ (Fig. SA and SB).

3.4 Triton X-100 micelles—structural characterization

As for the Igepal CA-520 systems, our first aim for the Triton X-100 systems was to find out if the size of the micelles could be easily correlated to the initial hydrogenation rate of DMI. The SANS measurements were analysed using the Guinier approximation, which generally gives estimates which are accurate to within 5–10% if the analysis is performed using data collected within the range where $qR_g \approx 1$, and provided that the particles studied are still so dilute that their interaction can be neglected.[19]

3.4.1 Scattering curves. Fig. 7 presents SANS scattering curves for four Triton microemulsions with $\omega = 20$ and different amounts δ of pentanol contained. All the curves show the existence of non-interactive particle systems and by comparing them one could suggest that the change of maximum height that increases with decreasing δ points to the increasing micellar size. The points of the scattering curves within the marked q range were used for Guinier approximation.

3.4.2 Guinier approximation. Linear regressions on Guinier plots ($\ln(I)$ *vs.* q^2) of the SANS data give access to the radius of the micelle, as shown in Fig. 8. The radius of gyration of the micelle was extracted from eqn (2) and it is equal to $\sqrt{3m}$, where m is the slope of the curve. The radius of the corresponding homogeneous sphere was obtained by using eqn (3). Fig. 9 summarizes the resulting radii for all the Triton X-100 microemulsions shown in Table 1. In this case the continuous and the internal phase were deuterated, so the sizes determined are the overall radii of gyration of the micelles. The four systems show tendencies which surpass the initial hydrogenation rates obtained with the biphasic system (4 mL_{H_2} min^{-1}).[6] When comparing the four systems with the same ω, the gyration radii of the micelles with different δ have similar tendencies. Only one system (ME 1 with $\omega = 20$, $\delta = 0.75$) stands out of the standard behaviour, with smaller amount of pentanol but larger amount of deuterium oxide. The comparison of the scattering curves for the four systems with $\omega = 20$, displayed in Fig. 7, gives a hint. By comparing the scattering curves of the four systems with $\omega = 20$, it is possible to identify the difference of this system, which shows a distinguishable characteristic curve for ellipsoidal micelles,[32,33] in which a smoother decrease of the intensity at mid q is observed. This could be caused by the penetration of solvent (cyclohexane or pentanol), originating a Gaussian distribution

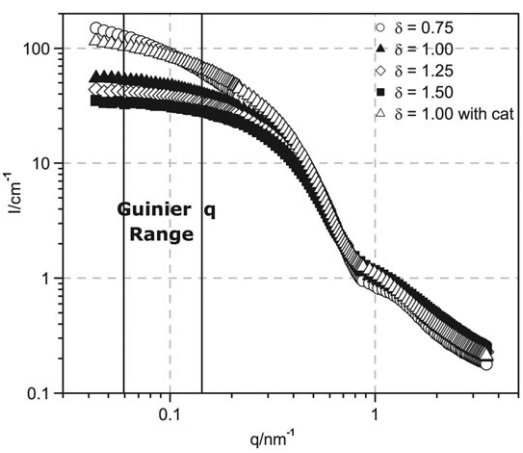

Fig. 7 SANS spectra of Triton X-100 microemulsions with $\omega = 20$ and different δ, and influence of the water-soluble catalyst complex Rh-TPPTS on the spectra.

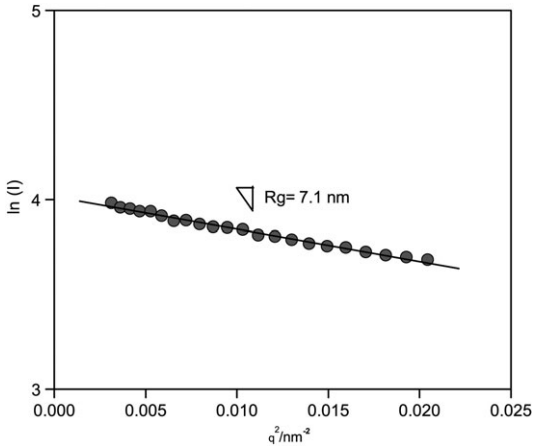

Fig. 8 Guinier plot of ln(I) *vs.* q^2 for the Triton X-100 microemulsion constituted by 4.17 g of water, 62.63 g of cyclohexane, 7.43 g of Triton X-100 and 7.43 g of 1-pentanol (ME 4 in Table 1), and corresponding fit.

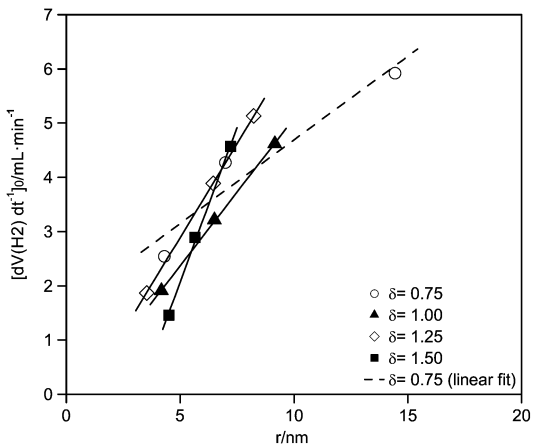

Fig. 9 Initial hydrogenation rate of the catalytic hydrogenation of DMI (2 g in 100 ml of microemulsion) as a function of the micelle radius of the homogeneous spheres (determined by Guinier approximation of the SANS spectra) in Triton X-100 microemulsions with different δ, at 25 °C and 1.1 bar, using 20 mg of $[Rh(cod)Cl]_2$ and 357 mg of TPPTS.

around the mean value of the radius.[34] This penetration of solvent is represented in Scheme 4 by molecules of cyclohexane in the interface of the micelle.

In order to obtain a preliminary study of the shape of the micelles which could serve as a first step for a deeper analysis of the micelles using specific models, the ratio V_{Sph}/V_{I_0} was calculated. The volume of the spherical micelles (V_{Sph}) was calculated with the Guinier approximation and V_{I_0} was estimated with the coherent macroscopic scattering cross section (see Tables SD and SE in ESI‡). The amount of pentanol inside the micelles increases the contrast and the volume fraction, which decreases the calculated volume of the micelles. For this reason and following the simplifications discussed from the resulting pentanol partitioning study, we assume no pentanol to be introduced inside the core of the micelles. With this assumption the two volumes are more similar. The results are shown in Table 3. As shown in Fig. 10a, the volume of the spherical micelles is similar to V_{I_0} when ω is smaller. We also calculated the ratio V_{Ellip}/V_{I_0}. The volume of the ellipsoidal micelles (V_{Ellip}) was calculated using the following equations for Guinier approximations:

$$R^2_{g_{Ellip}} = \tfrac{1}{5}(2a^2 + b^2)\ V_{Ellip} = \tfrac{4}{3}a^2 b \qquad (9)$$

where a and b are the short and long cross sections of the ellipsoidal micelle.

Guinier approximations are generally used at low q to obtain an estimation of the radius of the particles. Generally, the decay of the intensity at mid q for spherical particles is steeper than the one for ellipsoidal particles. This is because at mid q the shorter cross section of the ellipsoidal particles can be looked at. For this reason, a Guinier approximation at mid q for ellipsoidal particles allows for an estimation of the smaller radius and it was used to determine a. Using eqn (9), b and V_{Ellip} were obtained.

As seen in Fig. 10b, complemented with Table SF of the ESI,‡ the volume of the ellipsoidal micelles is similar to V_{I0} when ω is higher so both diagrams in Fig. 10 corroborate the tendency to form ellipsoids with higher amounts of water. The ellipticity was also calculated; it is the ratio between b and a. Fig. 11 shows a very small influence of the cosurfactant on the ellipticity of the micelles. A large ellipticity is observed with small amount of pentanol (δ = 0.75) and large amount of water (ω = 20), which reinforces the idea of solvent penetration.

3.4.3 Interface. As shown in Table 3, the radius obtained for the microemulsion ME 4 with deuterated core (deuterium oxide) calculated using the slope of the Guinier approximation for this sample is 7.1 nm. By comparing it to the 9.2 nm radius obtained for the same microemulsion ME 4 with deuterated core and cyclohexane-d_{12} as continuous phase, an acceptable interfacial surfactant layer of 2.1 nm thickness is estimated.[7] Dennis *et al.* calculated the fully extended length of the octylphenyl group using Corey–Pauling–Koltung models. They obtained a length smaller than 1 nm, so they assumed it to be 1 nm. They also calculated the length of the ethoxy chain, assuming it forms a random coil obtaining a length of 1.6 nm. Adding both parts, results are not so far from ours. The differences can be explained by the solvent penetration, which solvates the aliphatic chain of the surfactant. Because the interface and the continuous phase are diffuse, a defined boundary between interface and continuous phase is difficult to detect.

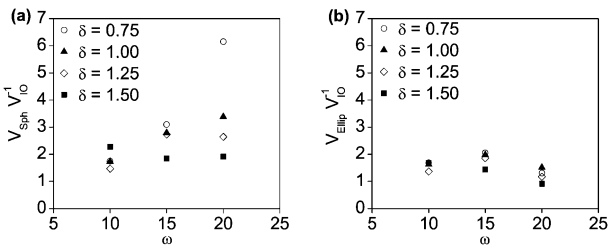

Fig. 10 Volume ratios of the Triton X-100 micelles with different δ, calculated with Guinier approximation as a function of ω assuming the micelles are: (a) spheres and (b) ellipsoids.

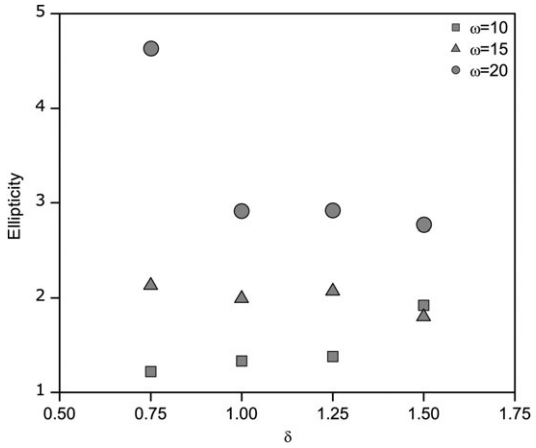

Fig. 11 Ellipticity of the Triton X-100 micelles as a function of δ.

3.4.4 Conductivity. The difference in geometry was also identified with the conductivity. The conductivity of a microemulsion is influenced by the microstructures of the micelles.[35] Oil-in-water microemulsions have similar conductivities to bulk water, and in water-in-oil microemulsions, the conductive polar phase is isolated by a continuous oil phase, therefore leading to small conductivities. Bicontinuous microemulsions show high conductivities, which decrease when the water content is lowered.[36] Water-in-oil microemulsions with small water contents show conductivities which decrease with the decrease in the surfactant concentration.[37] Independently of what the SANS measurements show, the presence of a maximum conductivity peak of 0.9 μS cm^{-1} in Fig. 12, when keeping $\omega = 20$ and changing the pentanol to Triton X-100 ratio (δ), identifies the existence of a different geometry of the microstructure, which could be reaching out, interacting with each other and creating some continuity. The maximum peak is obtained at $\delta = 0.70$. This is in agreement with the SANS data (Fig. 7) which indicate the presence of elongated micelles at $\delta = 0.75$, and elongated reverse micelles are expected to exhibit a higher conductivity compared to spherical micelles.

3.4.5 Effect of the catalyst incorporation. When adding the water-soluble catalyst complex (Rh–TPPTS) to the microemulsion ME 4, the SANS spectrum shows a different size, and similar to the microemulsion ME 1, a steeper decay for ME 4 at low q is observed (but not so pronounced as observed in Fig. 7 for ME 1). The radius of the catalyst containing micelles (C_{Rh} = 0.8 mmol L^{-1}) determined by Guinier approximation of the SANS spectra is 13.0 nm, which represents almost one and a half times the size of the empty micelles (r = 9.2 nm). This non-proportionate growth of the micelles is an indicator of the deformation of the micelles. The slight elongation of the micelles could be a result of the competition between the polar ethoxylated groups of the Triton X-100 molecules and the water-soluble catalyst complex Rh–TPPTS for the water molecules. Other important effects could be: the incorporation of the amphiphilic TPPTS into the interface or the interaction between the trivalent anion TPPTS and the ethoxy head groups. This effect should be stronger when δ is smaller: the 1-pentanol molecules distribute between the interfacial layers where they substitute Triton molecules and the oil rich bulk phase, thereby making the amphiphilic layers effectively more lipophilic, and in turn less interactive with the water molecules.[38,39] This behaviour could be the reason for the different tendencies shown in Fig. 5. A detailed study of the effect of the water-soluble catalyst complex on the Triton X-100 reverse micelles is a topic currently under research in our laboratory.

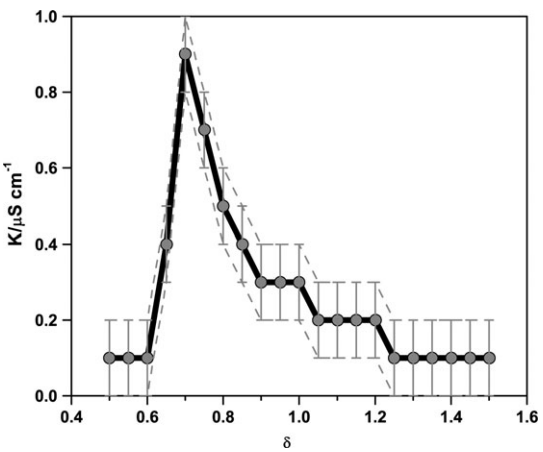

Fig. 12 Conductivity of 10% Triton X-100 microemulsions as a function of δ keeping $\omega = 20$ at 25 °C.

3. Conclusions

In order to improve the understanding of the mutual influence of the micelle microstructure on the catalytic hydrogenation of DMI when using microemulsions as a reaction medium, the structural dimensions of two octylphenyl-based microemulsions were studied and correlated with the catalytic hydrogenation of DMI performed in such media using the water-soluble catalyst complex Rh–TPPTS. The initial hydrogenation rate of DMI is proportional to the Rh–TPPTS concentrated Igepal CA-520 micelle radius, which was measured with DLS and also proportional to catalyst concentrated Triton X-100 micelle radius, determined from SANS spectra using Guinier approximations. The cosurfactant 1-pentanol plays an important role in the micelle size and shape of the Triton-based microemulsions, which at the same time influences the initial hydrogenation rate. The water-soluble catalyst complex Rh–TPPTS showed a complex influence on the shape and size of the Triton X-100 micelles and induces an elongation of the aggregates.

Acknowledgements

This work is part of the Cluster of Excellence "Unifying Concepts in Catalysis". Financial support by the Deutsche Forschungs-gemeinschaft (DFG) within the framework of the German Initiative for Excellence is gratefully acknowledged. The experiments at BENSC in Berlin were supported by the European Commission under the 6th Framework Programme through the Key Action: Strengthening the European Research Area, Research Infrastructures, Contract No. RII3-CT-2003-505925 (NMI3). A special thanks to Verena Strempel for all the hard work invested in the experiments.

J.M. is also grateful to the Deutscher Akademischer Austauschdienst (DAAD) and to the Fundación Gran Mariscal de Ayacucho (Fundayacucho) for receiving a doctoral scholarship.

References

1 G. Oehme, in *Aqueous-Phase Organometallic Catalysis*, ed. B. Cornils and W. A. Herrmann, Wiley-VCH, Weinheim, 2004, pp. 256–271.
2 D. Langevin, *Annu. Rev. Phys. Chem.*, 1992, **43**, 341–369.
3 J. Sjöblom and S. E. Friberg, in *Handbook of Microemulsion Science and Technology*, ed. P. Kumar and K. L. Mittal, Marcel Dekker, Inc, New York, 1999, pp. 833–842.
4 M. J. Schwuger, K. Stickdorn and R. Schomäcker, *Chem. Rev.*, 1995, **95**, 849–864.
5 T. Dwars, E. Paetzold and G. Oehme, *Angew. Chem., Int. Ed.*, 2005, **44**, 7174–7199.
6 J. S. Milano-Brusco, M. Schwarze, M. Djennad, H. Nowothnick and R. Schomäcker, *Ind. Eng. Chem. Res.*, 2008, **47**, 7586–7592.
7 R. J. Robson and E. A. Dennis, *J. Phys. Chem.*, 1977, **81**, 1075–1078.
8 S. M. Andrade and S. M. B. Costa, *Photochem. Photobiol. Sci.*, 2002, **1**, 500–506.
9 K. Wormuth, O. Lade, M. Lade and R. Schomäcker, in *Handbook of Applied Surface and Colloid Chemistry*, ed. K. Holmberg, John Wiley & Sons, West Sussex, 2001, pp. 605–627.
10 D. M. Zhu, K. I. Feng and Z. A. Schelly, *J. Phys. Chem.*, 1992, **96**, 2382–2385.
11 D. M. Zhu, X. Wu and Z. A. Schelly, *Langmuir*, 1992, **8**, 1538–1540.
12 M. Dvolaitzky, M. Guyot, M. Lagues, J. P. Lepesant, R. Ober, C. Sauterey and C. Taupin, *J. Chem. Phys.*, 1978, **69**, 3279–3288.
13 S. H. Chen, *Annu. Rev. Phys. Chem.*, 1986, **37**, 351–399.
14 S. H. Chen, J. Rouch, F. Sciortino and P. Tartaglia, *J. Phys.: Condens. Matter*, 1994, **6**, 10855–10883.
15 M. Gradzielski, D. Langevin and B. Farago, *Phys. Rev. E: Stat. Phys., Plasmas, Fluids, Relat. Interdiscip. Top.*, 1996, **53**, 3900–3919.
16 M. Gradzielski, D. Langevin and B. Farago, *Prog. Colloid Polym. Sci.*, 1996, **100**, 162–169.
17 M. Gradzielski, D. Langevin, T. Sottmann and R. Strey, *J. Chem. Phys.*, 1997, **106**, 8232–8238.
18 B. Abécassis, F. Testard, L. Arleth, S. Hansen, I. Grillo and T. Zemb, *Langmuir*, 2006, **22**, 8017–8028.
19 K. S. Freeman, N. C. B. Tan, S. F. Trevino, S. Kline, L. B. McGown and D. J. Kiserow, *Langmuir*, 2001, **17**, 3912–3916.
20 J. Oberdisse, O. Regev and G. Porte, *J. Phys. Chem. B*, 1998, **102**, 1102–1108.
21 G. Verma, V. K. Aswal, S. K. Kulshreshtha, P. A. Hassan and E. W. Kaler, *Langmuir*, 2008, **24**, 683–687.
22 E. Caponetti, A. Lizzio, R. Triolo, W. L. Griffith and J. S. Johnson, *Langmuir*, 1992, **8**, 1554–1562.
23 L. Garcia-Rio and P. Hervella, *Chem.–Eur. J.*, 2006, **12**, 8284–8295.
24 S. W. Provencher, *Comput. Phys. Commun.*, 1982, **27**, 213–227.
25 B. Hammouda, Probing Nanoscale Structures—The Sans Toolbox, http://www.ncnr.nist.gov/staff/hammouda/the_SANS_toolbox.pdf (November 2008).
26 M. Kahlweit and R. Strey, *Angew. Chem., Int. Ed. Engl.*, 1985, **24**, 654–668.
27 K. V. Schubert and E. W. Kaler, *Ber. Bunsen-Ges. Phys. Chem.*, 1996, **100**, 190–205.
28 M. Lade, H. Mays, J. Schmidt, R. Willumeit and R. Schomacker, *Colloids Surf., A*, 2000, **163**, 3–15.
29 S. P. Moulik and B. K. Paul, *Adv. Colloid Interface Sci.*, 1998, **78**, 99–195.
30 L. Garcia-Rio, J. C. Mejuto and M. Perez-Lorenzo, *New J. Chem.*, 2004, **28**, 988–995.
31 T. K. Jain, M. Varshney and A. Maitra, *J. Phys. Chem.*, 1989, **93**, 7409–7416.
32 O. Glatter, in *Neutrons, X-rays and Light: Scattering Methods Applied to Soft Matter*, ed. P. Lindner and T. Zemb, Elsevier Science B.V., Amsterdam, 2002, pp. 73–103.
33 C. Moitzi, N. Freiberger and O. Glatter, *J. Phys. Chem. B*, 2005, **109**, 16161–16168.
34 R. Strey, *Colloid Polym. Sci.*, 1994, **272**, 1005–1019.
35 M. Jonströmer, B. Jönsson and B. Lindman, *J. Phys. Chem.*, 1991, **95**, 3293–3300.
36 C. Cabaleiro-Lago, L. Garcia-Rio and P. Hervella, *Langmuir*, 2007, **23**, 9586–9595.
37 H. F. Eicke and J. C. Shepherd, *Helv. Chim. Acta*, 1974, **57**, 1951–1963.
38 M. Kahlweit, *J. Phys. Chem.*, 1995, **99**, 1281–1284.
39 Z. H. Luo, X. L. Zhan and P. Y. Yu, *Chin. Chem. Lett.*, 2004, **15**, 1101–1104.